Int. J. Heat Mass Transfer. Vol. 18, pp. 1455–1465. Pergamon Press 1975. Printed in Great Britain

THE DEVELOPMENT OF LAMINAR NATURAL-CONVECTIVE FLOW IN A VERTICAL UNIFORM HEAT FLUX DUCT

J. R. DYER*
The University of Adelaide, Adelaide, South Australia, 5001

(*Received* 1 *January* 1975 *and in revised form* 14 *March* 1975)

Abstract—An account of a theoretical and experimental study of laminar natural-convective flow in heated vertical ducts is presented. The ducts are open-ended and circular in cross-section and their internal surfaces dissipate heat uniformly.

Temperature and velocity fields and the relationship between Nusselt and Rayleigh numbers were obtained by solving the governing equations by a step-by-step numerical technique. Two Rayleigh numbers are introduced, one expressed in terms of the uniform heat flux and the other in terms of the mean wall temperature. The influence that the Prandtl number has on the relationship between the Nusselt and Rayleigh numbers is discussed. Three inlet conditions were examined; they all gave the same Nusselt relationship at small Rayleigh numbers and the differences between the Nusselt relationships obtained at large Rayleigh numbers were only small.

Experimentally determined Nusselt numbers, with air as the convected fluid, agreed satisfactorily with the theoretical relationship.

NOMENCLATURE

c_p, specific heat at constant pressure;
C, constant;
d, diameter of duct;
f, uniform surface heat flux;
F, dimensionless uniform heat flux, $1/Pr$;
g, acceleration of gravity;
Gr, Grashof number, $g\beta f r_w^5/\nu^2 l k$;
Gr_l, Grashof number, $g\beta f l^4/\nu^2 k$;
Gr^+, Gr/Nu;
h_x, heat dissipation (from inlet to elevation x);
H_x, dimensionless heat dissipation, $h_x/Raflr_w$ (from inlet to elevation X);
k, thermal conductivity;
l, length of duct;
L, dimensionless length, $1/Gr$;
Nu, Nusselt number, $fr_w/(T_{wm}-T_0)k$ or $1/\theta_{wm}$;
p, pressure;
P, dimensionless pressure, $pr_w^4/\rho l^2\nu^2 Gr^2$;
q, volume flow;
Q, dimensionless flow, $q/l\nu Gr$;
r, radial co-ordinate;
R, dimensionless radial co-ordinate, r/r_w;
Ra, Rayleigh number, $GrPr$;
Ra^+, Ra/Nu;
T, temperature;
u, velocity in x-direction;
U, dimensionless velocity in x-direction, $ur_w^2/l\nu Gr$;
v, velocity in r-direction;
V, dimensionless velocity in R-direction, vr_w/ν;
x, vertical co-ordinate;
X, dimensionless vertical co-ordinate, x/lGr.

Greek symbols

β, coefficient of thermal buoyancy;
θ, dimensionless temperature, $(T-T_0)k/fr_w$;
μ, dynamic viscosity;
ν, kinematic viscosity;
ρ, density.

Subscripts

c, axis of duct;
d, defect (pressure), diameter;
i, condition at inlet;
l, length of duct;
m, mean value;
me, mid-elevation;
o, ambient condition;
r, radius of duct;
t, top of duct;
w, wall of duct;
wm, wall, mean value;
wt, wall, top;
wx, wall, location;
x, elevation x or X.

INTRODUCTION

THERE is often the need to cool the internal surfaces of vertical open-ended ducts and of banks of tubes by natural convection, despite the low rates of heat transfer that this convective process affords. Thus information on the behaviour of natural-convective flow through confined spaces has wide use, which in recent years has included research and development in the diverse fields of nuclear and solar energy.

The investigation reported in the present paper deals with vertical circular ducts whose internal surfaces

*Senior Lecturer, Department of Mechanical Engineering.

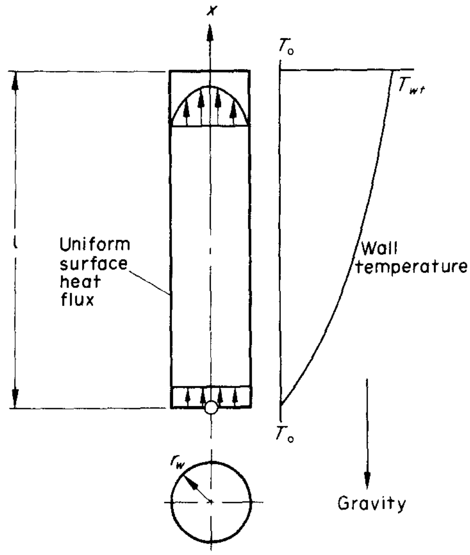

FIG. 1. Diagrammatic view of a vertical circular duct with a uniform surface heat flux.

dissipate heat uniformly. Such a duct is shown diagrammatically in Fig. 1. It will be seen that the natural-convective flow induced by the uniform surface heat flux produces temperatures on the wall that increase along the duct. Unlike the temperature distribution that occurs along a vertical flat surface with a uniform heat flux [1], the distribution of the temperature along the wall of the duct is not fixed but varies with the geometry of the duct and the heat flux.

The problem of laminar natural-convective flow through a confined space was first studied by Elenbaas [2, 3] and his initial work was concerned with the heated vertical channels formed by two parallel and infinitely wide flat plates [2]. Later Elenbaas established the heat dissipating characteristics of vertical ducts of circular and other cross-sectional shapes with uniform surface temperatures by transforming the results of his theoretical study of natural-convective flow through vertical parallel-plate channels [3]. However, it was not possible to obtain the temperature and velocity profiles in a duct by this method of solution. This significant short-coming of Elenbaas's method was remedied by Dyer [4], who used a finite difference technique to study the development of natural-convective flow in vertical circular ducts with uniform temperature and uniform flux heating. The method of solution was similar to that used by Bodoia and Osterle [5] in their study of natural-convective flow in a vertical channel formed by two parallel flat surfaces. Kageyama and Izumi [6], and Davis and Perona [7] also have reported on the development of the flow in uniform heat flux ducts for Prandtl numbers of 0·72 and 0·7 respectively.

There is clearly the need to extend the previous work on uniform heat flux ducts [4, 6, 7] and also to express some of the pertinent data in a more usable form. Consequently, the purpose of the present paper is to provide information on the relationship between the heat flux and the mean wall temperature; to discuss the effect of different inlet conditions on the theoretical solutions; to discuss the effect of Prandtl number on the Nusselt–Rayleigh number relationship; and to present simplified analyses of the relationship between Nusselt and Rayleigh numbers at small and large values of the Rayleigh number. In addition, the results of confirmatory experimental work are presented.

THEORY

Equations governing the flow

As shown diagrammatically in Fig. 1, the uniform flux heating of the wall of the duct produces a natural-convective flow with the fluid entering at the bottom and leaving at the top. Small density differences resulting from temperature gradients in the fluid give rise to the buoyancy forces producing the motion.

Throughout the analysis the following simplifying assumptions are made: fluid properties, except density, are independent of temperature; density variations are significant only in producing the buoyancy forces; and the flow is steady, laminar and incompressible, and axisymmetrical. Thus the well-known equations, in cylindrical co-ordinates, governing the flow are:

Continuity:

$$\frac{\partial u}{\partial x}+\frac{1}{r}\frac{\partial(rv)}{\partial r}=0 \tag{1}$$

Momentum:

$$\rho\left[u\frac{\partial u}{\partial x}+v\frac{\partial u}{\partial r}\right]=-\frac{\partial p}{\partial x}+\mu\left[\frac{1}{r}\frac{\partial}{\partial r}\left(r\frac{\partial u}{\partial r}\right)+\frac{\partial^2 u}{\partial x^2}\right]-\rho \boldsymbol{g} \tag{2}$$

$$\rho\left[u\frac{\partial v}{\partial x}+v\frac{\partial v}{\partial r}\right]=-\frac{\partial p}{\partial r}+\mu\left[\frac{\partial}{\partial r}\left(\frac{1}{r}\frac{\partial rv}{\partial r}\right)+\frac{\partial^2 v}{\partial x^2}\right] \tag{3}$$

Energy:

$$u\frac{\partial T}{\partial x}+v\frac{\partial T}{\partial r}=\frac{k}{\rho c_p}\left[\frac{\partial^2 T}{\partial r^2}+\frac{1}{r}\frac{\partial T}{\partial r}+\frac{\partial^2 T}{\partial x^2}\right]. \tag{4}$$

As the flow is confined, the pressure within the duct p, will be less than the hydrostatic pressure p_0, at the same elevation. The difference between the two pressures $p-p_0$, will be known as the pressure defect p_d, [5]. Since the hydrostatic pressure decreases with elevation according to

$$\frac{\mathrm{d}p_0}{\mathrm{d}x}=-\rho_0 \boldsymbol{g}. \tag{5}$$

Equation (2) can be rewritten as follows by introducing the coefficient of thermal buoyancy.

$$\rho\left[u\frac{\partial u}{\partial x}+v\frac{\partial u}{\partial r}\right]$$
$$=-\frac{\partial p_d}{\partial x}+\mu\left[\frac{1}{r}\frac{\partial}{\partial r}\left(r\frac{\partial u}{\partial r}\right)+\frac{\partial^2 u}{\partial x^2}\right]+\rho \boldsymbol{g}\beta(T-T_0). \tag{6}$$

Equations (1), (6), (3) and (4) can be expressed in the following dimensionless forms by introducing the dimensionless variables listed in the Nomenclature.

Thus

$$\frac{\partial U}{\partial X}+\frac{V}{R}+\frac{\partial V}{\partial R}=0 \quad (7)$$

$$U\frac{\partial U}{\partial X}+V\frac{\partial U}{\partial R}=-\frac{\partial P_d}{\partial X}+\frac{\partial^2 U}{\partial R^2}+\frac{1}{R}\frac{\partial U}{\partial R}+\theta \quad (8)$$

$$\frac{\partial P_d}{\partial R}=0 \quad (9)$$

$$U\frac{\partial \theta}{\partial X}+V\frac{\partial \theta}{\partial R}=\frac{1}{Pr}\left[\frac{\partial^2 \theta}{\partial R^2}+\frac{1}{R}\frac{\partial \theta}{\partial R}\right]. \quad (10)$$

It should be noted that terms that were multiplied by the factor $(r_w/lGr)^2$ have been omitted from the foregoing set of equations; this simplification was permissible because in most practical situations $(r_w/lGr)^2$ will be very much less than unity.

An additional governing equation is provided by the fact that for negligible changes in density the volume flow is constant throughout the duct. Thus the dimensionless volume flow Q, at all elevations is given by

$$Q=2\pi\int_0^1 U_x R\,\mathrm{d}R. \quad (11)$$

General Nusselt relationship

The rate of heat transfer H_x, from the bottom of the duct to elevation X is

$$H_x=2\pi\int_0^1 U_x\theta_x R\,\mathrm{d}R \quad (12)$$

or in terms of the dimensionless heat flux F,

$$H_x=2\pi XF. \quad (13)$$

The overall dimensionless rate of heat transfer H_t, by definition, is

$$H_t=\frac{h_t}{Raflr_w} \quad (14)$$

and if h_t is replaced by $2\pi r_w lf$ equation (14) reduces to

$$H_t=\frac{2\pi}{Ra}. \quad (15)$$

Dividing equation (15) by the dimensionless surface area $2\pi L$, and replacing L by $1/Gr$ (by definition $L=1/Gr$) shows that the dimensionless heat flux F, reduces to the reciprocal of the Prandtl number, that is

$$F=\frac{1}{Pr}. \quad (16)$$

Since the surface temperature varies along the duct, the reference temperature adopted for expressing the overall Nusselt number was the mean surface temperature [1], which is given by

$$T_{wm}=\frac{\int_0^l (T_{wx}-T_o)\,\mathrm{d}x}{l}. \quad (17)$$

Thus the overall Nusselt number of the duct (based on the mean surface temperature and the radius of the duct) is

$$Nu=\frac{fr_w}{(T_{wm}-T_o)k}. \quad (18)$$

Comparing equation (18) with the expression for the dimensionless mean surface temperature θ_{wm}, (from the definition of θ, $\theta_{wm}=(T_{wm}-T_o)k/fr_w$) shows that

$$Nu=\frac{1}{\theta_{wm}}. \quad (19)$$

The important relationship between the Nusselt and Rayleigh numbers was obtained by solving equations (7)–(11) simultaneously for the following boundary conditions.

Boundary conditions

Location	U	V	θ	P_d
$X=0, R=1$	$U=0$	$V=0$	$\theta=0$	*
$X=0, 0\leqslant R<1$	*	$V=0$	$\theta=0$	*
$0<X<L, R=1$	$U=0$	$V=0$		$P_d<0$
$0<X<L, R=0$		$V=0$		$P_d<0$
$X=L, R=1$	$U=0$	$V=0$		$P_d=0$
$X=L, R=0$		$V=0$		$P_d=0$

*Information on the inlet conditions follows.

In previous work [4, 6, 7] the pressure defect at both inlet and exit was taken to be zero. The assumption that the pressure defect at inlet is zero is, however, open to criticism [8] because it ignores even the pressure drop that induces the fluid in the environment to flow to the inlet. Therefore, in order to study the effect that the inlet condition has on the rate of heat transfer the following inlet conditions were considered:

(a) Uniform velocity with a zero pressure defect at inlet.
(b) Uniform velocity with a pressure drop produced by acceleration of the fluid from rest. Under these circumstances the pressure defect at inlet, from Bernoulli's equation, is

$$P_{di}=-\frac{U_i^2}{2}. \quad (20)$$

(c) Parabolic velocity profile with a pressure drop produced by the acceleration of the fluid from rest. For this condition the mean pressure defect at inlet is

$$P_{di}=-\frac{\pi}{Q}\int_0^1 U_i^3 R\,\mathrm{d}R. \quad (21)$$

It should be noted, however, that in a real situation the pressure drop at inlet is determined by the flow pattern induced in the fluid approaching the bottom of the duct.

Although hitherto it has been implied that the uniform heat flux f, is known, this may not always be the case. In fact, in practice, only temperatures along the wall may be available. Therefore, to meet this situation Nusselt relationships will also be established for known wall temperatures.

Before beginning the general solution, simplified solutions for small and large Rayleigh numbers will be obtained. These solutions, although only approximate, provide useful data against which the computed results can be checked.

Nusselt relationship for small Rayleigh numbers

As the Rayleigh number is defined as

$$Ra = \frac{g\beta f r_w^5}{v^2 l k} . Pr \tag{22}$$

small Rayleigh numbers can be obtained by making the ratio l/r_w sufficiently large. Further, since the mean temperature of the fluid at any elevation will lag behind that of the wall with uniform flux heating, fully developed flow conditions are not produced as in a uniform temperature duct [4, 6, 7, 9]. However, in this simplified analysis, the flow will be assumed to be fully developed and temperatures uniform across the duct. Thus the dimensionless vertical component of the velocity U at a radius R is approximately

$$U = 2Q(1-R^2)/\pi \tag{23}$$

and the dimensionless temperature of the fluid θ, at elevation X

$$\theta_x = \theta_{wx} \tag{24}$$

where θ_{wx} is the dimensionless temperature of the wall. For flow that is almost fully developed, the momentum equation, equation (8), reduces to

$$\frac{\partial P_d}{\partial X} = \frac{\partial^2 U}{\partial R^2} + \frac{1}{R}\frac{\partial U}{\partial R} + \theta. \tag{25}$$

Substituting equations (23) and (24) into equation (25) yields

$$\frac{\partial P_d}{\partial X} = \theta_{wx} - 8Q/\pi. \tag{26}$$

With a uniform heat flux and a velocity profile that does not change, θ_{wx} will increase linearly up the duct; and hence from equation (26) since Q is constant, $\partial P_d/\partial X$ will also increase linearly. Furthermore, if the pressure defect P_d, is zero at both the inlet and the exit, $\partial P_d/\partial X$ will change sign at mid-elevation. Also at mid-elevation, the temperature of the wall θ_{me}, will be approximately equal to the mean wall temperature θ_{wm}. Hence equation (26) at mid-elevation reduces to

$$\theta_{wm} = 8Q/\pi. \tag{27}$$

Considering now the heat dissipated by the wall, the dimensionless rate at which the lower half of the duct loses heat H_{me}, is given approximately by

$$H_{me} = Q\theta_{wm}. \tag{28}$$

Using equation (28), equation (27) becomes

$$\theta_{wm} = \sqrt{(8H_{me}/\pi)}. \tag{29}$$

Since the heat flux is uniform along the duct

$$H_{me} = H_t/2. \tag{30}$$

From equations (15) and (30)

$$H_{me} = \pi/Ra \tag{31}$$

and substituting equation (31) into equation (29) gives

$$\theta_{wm} = \sqrt{(8/Ra)}. \tag{32}$$

Finally, substituting equation (32) into equation (19) yields the following Nusselt relationship for small Ra

$$Nu = \sqrt{\left(\frac{Ra}{8}\right)}. \tag{33}$$

To obtain the Nusselt relationship based on the mean wall temperature, the following Grashof number Gr^+, incorporating the mean wall temperature [1] will be used.

$$Gr^+ = Gr/Nu = g\beta(T_{wm} - T_o)r_w^4/v^2 l. \tag{34}$$

Thus

$$Ra^+ = Ra/Nu. \tag{35}$$

Introducing equation (35) into equation (33) yields the following relationship for small Ra^+

$$Nu = Ra^+/8. \tag{36}$$

Nusselt relationship for boundary-layer flow

The other situation for which an estimate of the Nusselt number can be obtained is where the duct has a small value of l/r_w and consequently a large value of Ra. With a small value of l/r_w, it is reasonable to assume that the temperature and velocity distributions near the wall will be similar to those in the laminar natural-convective boundary layer on a flat surface. Hence, if the duct were to be opened out to form a vertical flat surface, there should be very little difference between the rate of heat transfer from the flat surface thus formed and the duct. Nu, therefore, has to be independent of the radius of the duct, and this requirement is achieved if

$$Nu = C(Ra)^{1/5} \tag{37}$$

where C is constant. If both sides of equation (37) are multiplied by l, the length of the duct, the following equation is obtained, which does not contain r_w, the radius,

$$Nu_l = C(Ra_l)^{1/5} \tag{38}$$

where the subscript l indicates that the length of the duct has become the characteristic dimension. Now the relationship for a vertical flat surface dissipating a uniform heat flux [1] for $Pr = 0{\cdot}7$ is

$$Nu_l = 0{\cdot}62(Ra_l)^{1/5} \tag{39}$$

and this equation will be seen to have the same form as equation (38). Hence, if C in equation (37) is assumed to be 0·62 also, the Nusselt relationship for laminar boundary-layer flow in the duct is approximately

$$Nu = 0{\cdot}62(Ra)^{1/5}. \tag{40}$$

To obtain the Nusselt relationship based on the mean wall temperature for boundary-layer flow, equation (35) is introduced into equation (40); thus

$$Nu = 0{\cdot}55(Ra^{+})^{1/4}. \tag{41}$$

It is interesting to compare equations (36) and (41) with the equivalent equations for uniform temperature ducts. Whereas equation (36) for small Rayleigh numbers gives a Nusselt number that is twice as large as the Nusselt number for the equivalent uniform temperature duct [4, 9], the Nusselt numbers for uniform heat flux and uniform temperature ducts at large Rayleigh numbers [4, 9] are almost the same.

Method of solving the flow equations

In order to obtain the relationship between the Nusselt and Rayleigh numbers for laminar flow, and to study the development of the flow in the duct, equations (7)–(11) were solved simultaneously on a high-speed digital computer.

Since laminar flow in a uniform surface heat flux duct is unidirectional, the equations were solved by a step-by-step relaxation technique similar to that described by Bodoia [10]. The assumption that the flow was axisymmetrical allowed the relaxation to take place on a two-dimensional grid containing the axis and a radial line. With this method, each row of the grid was relaxed in turn for the unknown values, including the wall temperature, beginning at the bottom of the duct.

Each solution was computed for a given Prandtl number and a dimensionless flow rate Q, beginning from an assumed inlet condition. The dimensionless length of the duct L, was established by continuing the relaxation until the pressure defect P_d, ceased to be negative. The reciprocal of the dimensionless length, by definition, gave the Grashof number, and substitution of the mean wall temperature θ_{wm}, into equation (19) gave the Nusselt number.

The finite difference forms of equations (7)–(10) are presented in Appendix A and the method of solution is described in Appendix B. Since air is the fluid in many natural-convective processes, most of the computations were for $Pr = 0{\cdot}7$.

Theoretical results

Nusselt relationships for Rayleigh numbers based on the uniform heat flux Ra, and on the mean wall temperature Ra^{+}, are shown in Figs. 2 and 3 respectively. From Fig. 2 the mean wall temperature of a duct with a known heat flux can be obtained, and from Fig. 3 the magnitude of the uniform heat flux for a known mean wall temperature. Both these figures were computed for a uniform velocity and a pressure defect of zero at inlet.

The effect of varying the Prandtl number of the fluid is shown in Fig. 2. Prandtl numbers greater than 0·7 are seen to have a negligible effect on the Nusselt–Rayleigh number relationship. On the other hand, for Prandtl numbers less than 0·7, Fig. 2 shows that the simple relationship $Nu = f(Ra)$, not surprisingly, ceases to hold [1], and that the Nusselt number is a function of both the Rayleigh number and the Prandtl number.

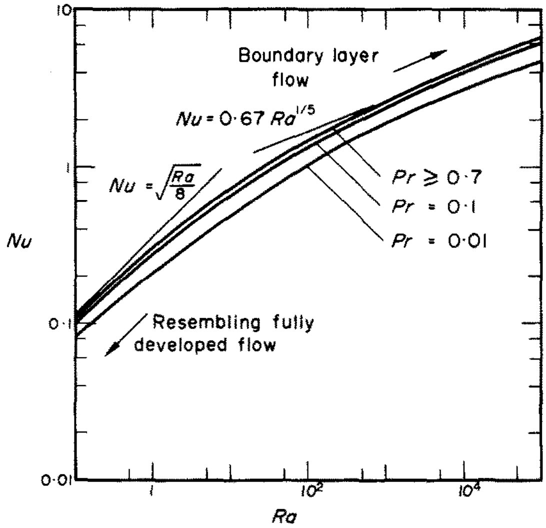

FIG. 2. The relationship between Nusselt number and Rayleigh number (based on the uniform heat flux) for a vertical circular duct with a uniform heat flux; the inlet velocity U_i, is uniform and the inlet pressure defect P_{di}, zero.

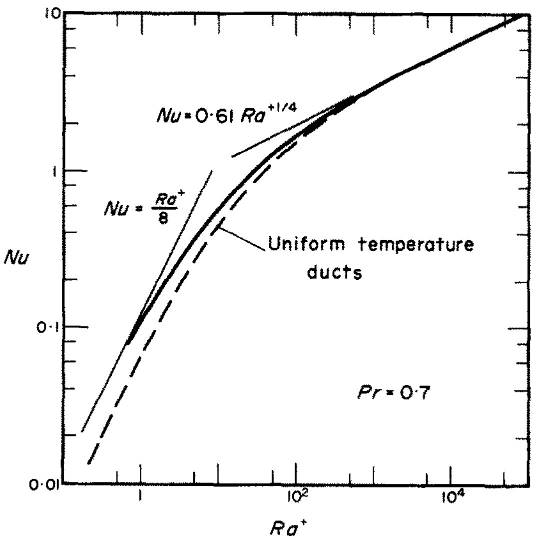

FIG. 3. The relationship between Nusselt number and Rayleigh number (based on the mean surface temperature) for a vertical duct with a uniform surface heat flux; inlet velocity U_i, is uniform and the inlet pressure defect P_{di}, zero.

The approximate Nusselt relationships derived for small and large Rayleigh numbers, equations (33) and (40) and equations (36) and (41), will be seen to agree satisfactorily with the asymptotic relationships shown in Figs. 2 and 3.

Figure 4 shows the effect of three inlet conditions on the Nusselt relationship. It will be seen that the effect is negligible at small Rayleigh numbers, and the maximum variation between the Nusselt numbers obtained at $Ra = 10^5$ is only 15 per cent. The negligible effect below $Ra = 100$ is understandable because below this Rayleigh number developed flow is approached in the lower part of the duct irrespective of the inlet conditions. It should be noted that although at large

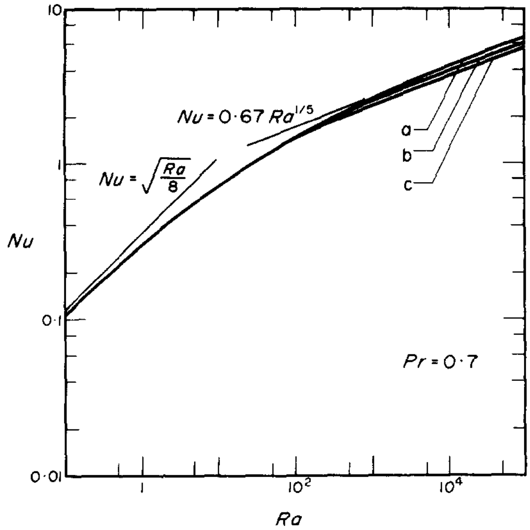

FIG. 4. The relationship between Nusselt number and Rayleigh number (based on the uniform heat flux) for a vertical duct with a uniform surface heat flux for the following inlet conditions: (a) U_i is uniform and $P_{di} = 0$; (b) U_i is uniform and $P_{di} = -(U_i^2/2)$; (c) U_i is parabolic and $P_{di} = -\frac{\pi}{Q}\int_0^1 U_i^3 R\,dR$.

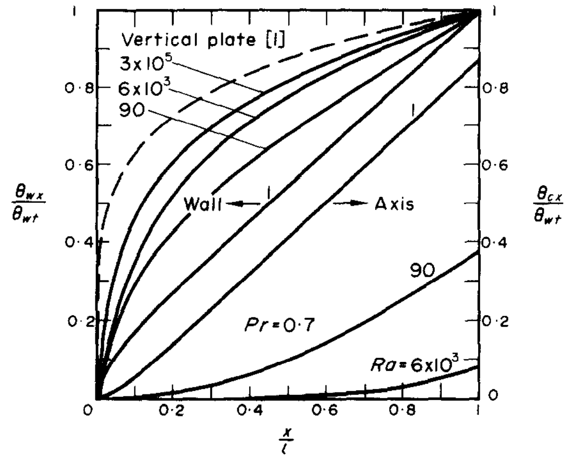

FIG. 5. Dimensionless temperatures along the surface θ_{wx}, and the centre line θ_{cx}, in terms of the wall temperature at the top of the duct θ_{wt}, for uniform heat flux ducts; the inlet velocity U_i, is uniform and the inlet pressure defect P_{di}, zero. The temperature along a vertical flat plate [1] is shown for comparison.

Rayleigh numbers the different inlet conditions produce only a small variation in the Nusselt relationship, their effect on the behaviour of the flow within the duct, as will be shown later, is quite marked.

It is interesting to note that Kageyama and Izumi [6], and Davis and Perona [7] each adopted a different way of presenting the Nusselt relationships to those shown in Figs. 2 and 3. Kageyama and Izumi [6] plotted, for various dimensionless flow volumes, local Nusselt numbers and mean Nusselt numbers against the dimensionless distance from the bottom of the duct X, while Davis and Perona [7] plotted local Nusselt numbers against the parameter $x/Re_d Pr\,d$ (which is equivalent to $\pi X/4Q\,Pr$) for comparison with the work of Kays [11] on forced convection in the entry region. In the present work, it will be recalled, the Nusselt number has been based on the mean wall temperature. This reference temperature is considered to have a greater practical relevance than any actual temperature on the wall because the latter could be distorted by a small variation in the uniformity of the heat flux. The desirability of using the mean wall temperature as the reference temperature was borne out when conducting the experimental work, which is reported in the following section.

Figure 5 compares the dimensionless temperatures along the wall θ_{wx}, with those along the axis of the duct θ_{cx}. It will be observed that for small Rayleigh numbers both temperatures are similar and increase almost linearly, and for large Rayleigh numbers the temperature distribution on the wall approaches that of a vertical flat plate with a uniform heat flux [1].

Figures 6 and 7 show the growth of the temperature and velocity profiles for various inlet conditions in ducts with a small and a large value of the Rayleigh

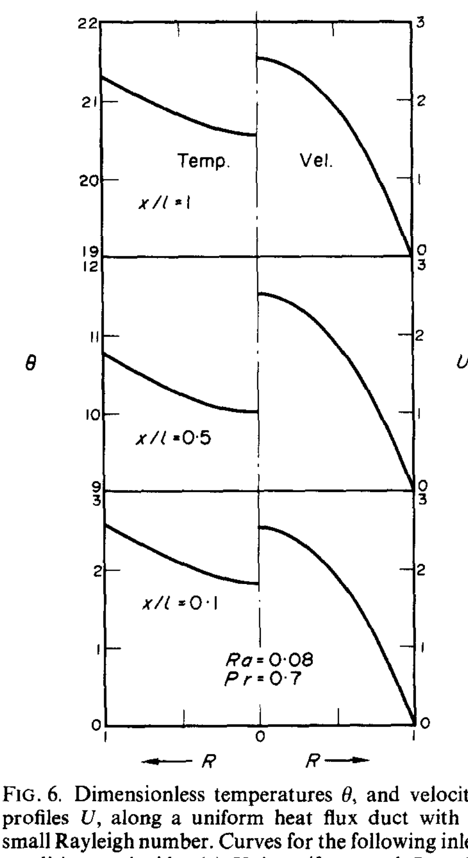

FIG. 6. Dimensionless temperatures θ, and velocity profiles U, along a uniform heat flux duct with a small Rayleigh number. Curves for the following inlet conditions coincide: (a) U_i is uniform and $P_{di} = 0$; (b) U_i is uniform and $P_{di} = -(U_i^2/2)$; (c) U_i is parabolic and $P_{di} = -\frac{\pi}{Q}\int_0^1 U_i^3 R\,dR$.

number respectively. For the small Rayleigh number temperature and velocity profiles that resemble fully developed flow are established near the bottom of the duct. On the other hand, for the large Rayleigh number Fig. 7 shows that boundary-layer flow is established

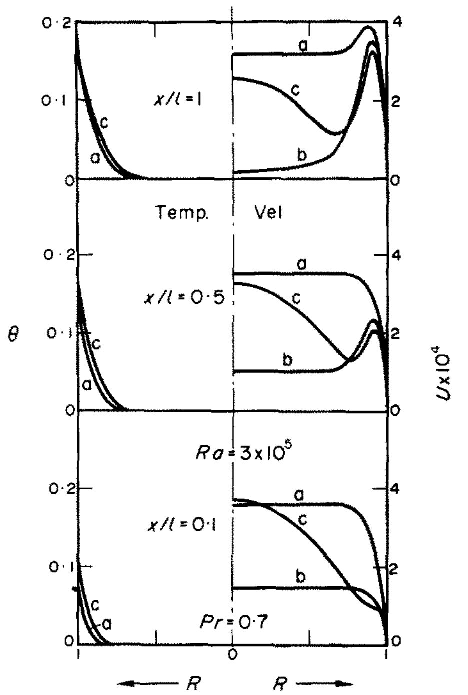

FIG. 7. Dimensionless temperature θ, and velocity profiles U, along a uniform heat flux duct with a large Rayleigh number for the following inlet conditions: (a) U_i is uniform and $P_{di} = 0$; (b) U_i is uniform and $P_{di} = -(U_i^2/2)$; (c) U_i is parabolic and

$$P_{di} = -\frac{\pi}{Q}\int_0^1 U_i^3 R\,\mathrm{d}R.$$

with a diminishing core of fluid that is not heated even at the top of the duct. This unheated core provides the fluid that flows into the growing boundary layer that develops adjacent to the wall. In the case of the low Rayleigh number the three inlet conditions will be seen in Fig. 6 to have no noticeable effect on the temperature and velocity profiles at and above $x/l = 0{\cdot}1$. In contrast, the effect of the inlet conditions on the velocity profiles for the large Rayleigh number is most marked at all elevations, although the temperature profiles, which hug the wall throughout, were not influenced to nearly the same extent. The similarity of the temperature profiles and the fact that the velocity profiles at the top of the duct are very similar near the wall accounts for the small effect that the inlet conditions have on the Nusselt relationship at large Rayleigh numbers as shown in Fig. 4.

The observations of Currie and Newman [12] in their experimental investigation into natural-convective flow through a vertical flat-plate channel suggest that a uniform inlet velocity is a reasonable assumption for a theoretical investigation. Furthermore, for the fluid to be induced to flow into the duct, the pressure at the inlet has to be lower than that of the surroundings at the same elevation. Consequently, the most realistic of the three inlet conditions is condition (b), which specifies both a uniform inlet velocity and a pressure defect at inlet.

Pressure defects along ducts with a small and a large Rayleigh number are shown in Fig. 8. In the case of the duct with the small Rayleigh number, the pressure defect curve is approximately parabolic and consequently the pressure gradient is almost linear, and zero at mid-elevation. This behaviour of the pressure defect was anticipated, it will be recalled, in deriving equation (33) for small values of the Rayleigh number. Inspection of Fig. 8 will show that the inlet conditions exert a much greater influence on the pressure defect at the large Rayleigh number.

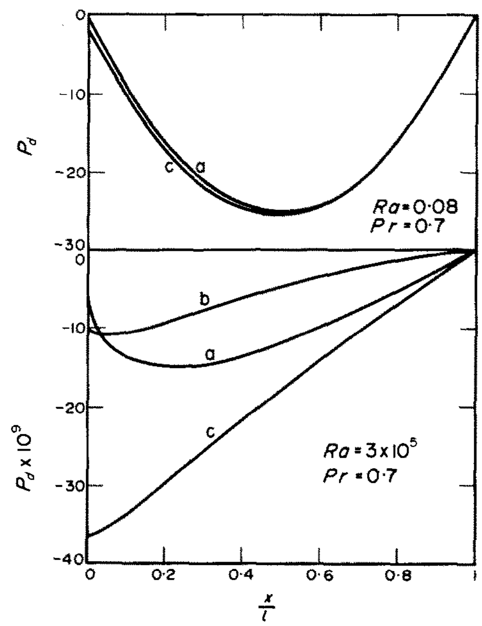

FIG. 8. Dimensionless pressure defects along uniform heat flux ducts for a small and a large Rayleigh number for the following inlet conditions: (a) U_i is uniform and $P_{di} = 0$; (b) U_i is uniform and $P_{di} = -(U_i^2/2)$; (c) U_i is parabolic and

$$P_{di} = -\frac{\pi}{Q}\int_0^1 U_i^3 R\,\mathrm{d}R.$$

For the small Rayleigh number the curve for inlet condition (b) (not shown) lies between curves (a) and (c).

In Fig. 9 the dimensionless volume Q, and the dimensionless overall rate of heat transfer H_t, are plotted against Rayleigh number for $Pr = 0{\cdot}7$. Unlike the corresponding parameters for the uniform surface temperature duct [4, 6, 7, 9] Q and H_t do not asymptotically approach a common value at small Rayleigh numbers. In fact, Q for small Ra will be seen to approach the relationship obtainable from equations (27) and (32), namely

$$Q = \frac{\pi}{\sqrt{(8Ra)}} \tag{42}$$

and H_t for all Ra to be inversely proportional to Ra in accordance with equation (15).

The behaviour of Q and H_t with Ra shown in Fig. 9 agrees with data presented by Davis and Perona [7]. However, their plot of Q, by not extending beyond $Ra = 10^3$, is misleading in that it suggests that Q varies inversely with $\sqrt{(Ra)}$ for all values of Ra instead of, as Fig. 9 shows, for only small values of Ra.

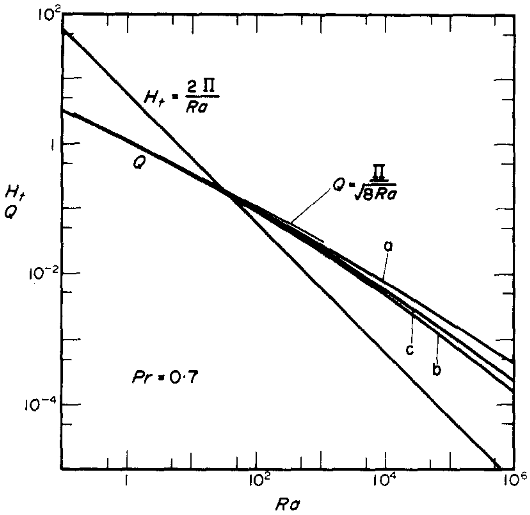

FIG. 9. Dimensionless flow Q, and overall heat transfer H_t, for uniform surface heat flux ducts plotted against Rayleigh number for the following inlet conditions: (a) U_i is uniform and $P_{di} = 0$; (b) U_i is uniform and $P_{di} = -(U_i^2/2)$; (c) U_i is parabolic and

$$P_{di} = -\frac{\pi}{Q}\int_0^1 U_i^3 R\,\mathrm{d}R.$$

Curve of dimensionless flow Q, by Davis and Perona [7] extends from $Ra = 1{\cdot}5$ to 700 and coincides with curve (a).

The dimensionless mean wall temperature θ_{wm}, and temperature of the wall at the top of the duct θ_{wt}, are shown in Fig. 10 plotted against the Rayleigh number. At small Rayleigh numbers the dimensionless mean wall temperature is about one-half of the dimensionless

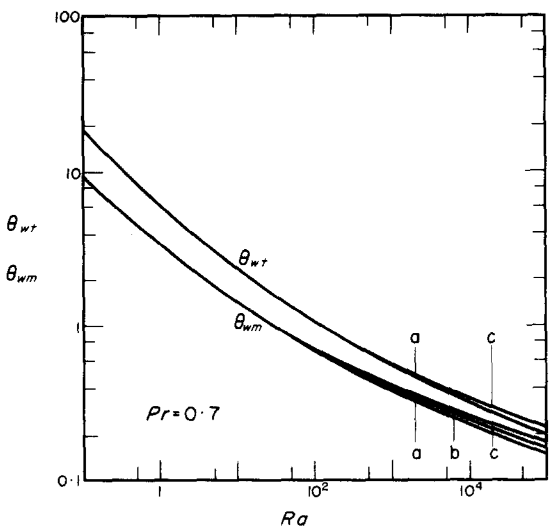

FIG. 10. Dimensionless temperature on the wall at the top of the duct θ_{wt}, and dimensionless mean wall temperature θ_{wm}, for uniform heat flux ducts plotted against Rayleigh number for the following inlet conditions: (a) U_i is uniform and $P_{di} = 0$; (b) U_i is uniform and $P_{di} = -(U_i^2/2)$; (c) U_i is parabolic and

$$P_{di} = -\frac{\pi}{Q}\int_0^1 U_i^3 R\,\mathrm{d}R.$$

In the case of θ_{wt} the curve for inlet condition (b) (not shown) lies between curves (a) and (c).

temperature at the top of the duct; this fact, it will be recalled, is consistent with the predictions made in establishing equation (33). However, as the Rayleigh number is increased it will be seen that the ratio of θ_{wm} to θ_{wt} becomes larger than a half. This relationship between θ_{wm} and θ_{wt} with Ra can be readily explained by examining the shape of the curves of θ_{wx}/θ_{wt} in Fig. 5.

EXPERIMENTAL STUDY

Since the theory was based on an ideal fluid whose properties, except for density in producing the buoyancy forces, were independent of temperature, it was considered desirable to conduct experiments in order to test the validity of at least part of the theoretical analysis. Consequently, with air as the working fluid experiments were carried out for Rayleigh numbers between 1 and 3000. This interval was considered interesting because it fell between the two extreme flow regimes for which additional theoretical information was available for corroboration, namely equations (33) and (40).

In order to span this range of Rayleigh numbers satisfactorily three ducts of different sizes were used. The ducts were 19·1, 25·4 and 46·7 mm in internal diameter and were all 1·22 mm long. Each duct was a thin-wall stainless steel tube and was heated by five, independently adjustable, electrical resistance elements. The elements were made of nichrome wire, helically wound around the external surface of the tube and positioned end-for-end along it. The external heat loss was minimised by insulating the exterior of the tube with fibre-glass, which was wrapped around it to a radial thickness of 150 mm. Fourteen thermocouples were embedded in the wall of the tube to monitor temperatures along the internal surface.

The difficulty of measuring small heat fluxes was overcome by the expedient of accepting the theoretically established distributions of wall temperature (shown in Fig. 5). With this compromise it was possible to obtain uniform flux heating by simply controlling the wall temperatures. Thus temperatures along the wall were matched, by adjusting the current in each of the five heating elements, with the theoretical temperature profile. Despite the thickness of insulation surrounding the tube, the external heat loss was comparable with the heat dissipated by the internal surface and therefore had to be taken into account. The heat loss was established by a similar heating of the duct with its ends closed and the difference between the two heat inputs gave a reasonable approximation to the heat dissipated by the internal surface itself. This method of determining the external heat loss is justified by the fact that owing to the air in the blocked duct increasing in an upward direction a stable situation was created with negligible air movements.

Even with five independently adjustable heating elements, it was not possible to obtain exactly the desired temperatures at the extremities of the duct. However, these deficiencies were of minor consequence since the mean wall temperature was used as the reference temperature for calculating the Nusselt number.

The properties of air used in the Nusselt and Rayleigh numbers were established in the following manner; the coefficient of thermal buoyancy was evaluated at ambient temperature and all other properties at the mean wall temperature.

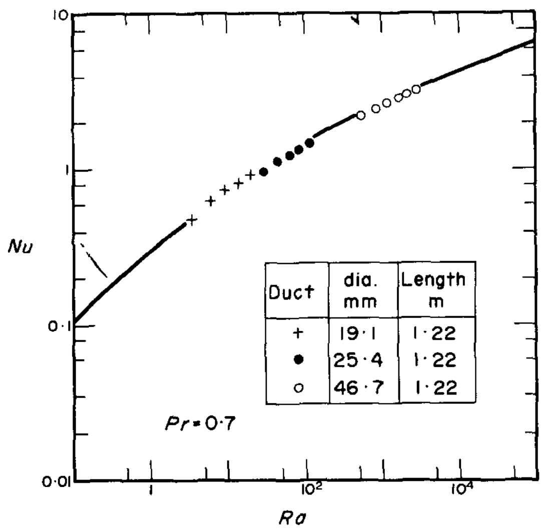

FIG. 11. Experimentally determined Nusselt numbers vs Rayleigh numbers. The convected fluid was air. The theoretical curve for $Pr = 0{\cdot}7$ from Fig. 2 is shown for comparison.

The experimentally determined Nusselt numbers are presented in Fig. 11; they will be seen to agree satisfactorily with the theory. It is interesting to note that although the experiments were conducted in a closed room within a large draught shield, the flow approaching the inlet, made visible by smoke, was neither steady nor axisymmetrical owing to the disturbing influence of very small air movements in the room. The fact that with these inlet conditions the experiments yielded overall Nusselt numbers that agreed with the theory corroborates the theoretical finding that the inlet conditions, within reason, are not important parameters in the range of Rayleigh numbers investigated experimentally.

CONCLUSIONS

In this analysis of the problem of natural-convective flow in a uniform heat flux duct the step-by-step numerical method has proved to be useful and flexible. Of considerable importance was the fact that the technique readily lent itself to investigating different boundary conditions.

In order to facilitate the practical use of the data that have been established, the Nusselt number was based on the mean wall temperature. Furthermore, Nusselt–Rayleigh number relationships have been presented in such a way that either the mean wall temperature can be ascertained from a known uniform heat flux or vice versa.

From the theoretical investigation the following conclusions can be drawn:

1. For Rayleigh numbers less than one the flow resembles fully developed flow and the Nusselt number varies with the square root of the Rayleigh number based on the uniform heat flux. For Rayleigh numbers greater than 1000 boundary-layer flow is produced and the Nusselt number varies with the fifth root of the Rayleigh number based on the uniform heat flux.
2. The Nusselt number for Prandtl numbers greater than or equal to 0·7 is a function of the Rayleigh number alone; however, for Prandtl numbers less than 0·7 the Prandtl number also enters the relationship.
3. The relationship between the overall Nusselt number and the Rayleigh number is relatively insensitive to small changes in the inlet conditions.

Although the theory was developed for an ideal fluid, the experiments with air yielded data that agreed satisfactorily with the theoretical relationship between Nusselt and Rayleigh numbers. This indicates that the theory would be applicable to other fluids whose properties do not vary too markedly with temperature.

It would be interesting to extend the experimental work into the higher Rayleigh number range where the effects of different inlet conditions become more pronounced. However, for the results to be of any real value the flow pattern at inlet would have to be established and the theoretical results re-computed accordingly for comparison.

Acknowledgements—This work was carried out in the Department of Mechanical Engineering at the University of Adelaide under the aegis of Professor R. E. Luxton. The advice given by Dr. J. Mannam and the assistance rendered by several students in carrying out the experimental work are gratefully acknowledged. Financial support for the project was provided by the Australian Institute of Nuclear Science and Engineering.

REFERENCES

1. E. M. Sparrow and J. L. Gregg, Laminar free convection from a vertical plate with a uniform heat flux, *Trans. Am. Soc. Mech. Engrs* **78**, 435–440 (1956).
2. W. Elenbaas, Heat dissipation of parallel plates by free convection, *Physica, s'Grav.* **9**, 1–28 (1942).
3. W. Elenbaas, The dissipation of heat by free convection (from) the inner surface of vertical tubes of different shapes of cross-section, *Physica, s'Grav.* **9**, 865–874 (1942).
4. J. R. Dyer, The development of natural convection in a vertical circular duct, *Mech. Chem. Engng, Trans. Instn Engrs Aust.* **MC4**, 78–86 (1968).
5. J. R. Bodoia and F. J. Osterle, Development of free convection between heated vertical plates, *J. Heat Transfer* **84**, 40–44 (1962).
6. M. Kageyama and R. Izumi, Natural heat convection in a vertical circular tube, *Bull. J.S.M.E.* **13**, 382–394 (1970).
7. L. P. Davis and J. P. Perona, Development of free convection flow of a gas in a heated vertical open tube, *Int. J. Heat Mass Transfer* **14**, 889–903 (1971).
8. T. Aihara, Effects of inlet boundary-conditions on numerical solutions of free convection between vertical parallel plates, *Rep. Inst. High Speed Mech., Tōhoku Univ.* **28**, 1–27 (1973).

9. J. R. Dyer, The development of laminar natural-convective flow in a vertical duct of circular cross-section that has a flow restriction at the bottom, *Heat Transfer 1970*, Vol. 4, Paper NC 2-8. Elsevier, Amsterdam (1970).
10. J. R. Bodoia, The finite difference analysis of confined viscous flow, Ph.D. Thesis, Carnegie Institute of Technology, Pittsburgh (1959).
11. W. H. Kays, Numerical solution for laminar flow in circular tubes, *Trans. Am. Soc. Mech. Engrs* 71, 1265–1274 (1955).
12. I. G. Currie and W. A. Newman, Natural convection between isothermal vertical surfaces, *Heat Transfer 1970*, Vol. 4, Paper NC 2-7. Elsevier, Amsterdam (1970).

APPENDIX A

Finite Difference Equations

Since the flow in the duct was assumed to be axisymmetrical, the relaxation was performed on a two-dimensional rectangular grid containing the axis and a radial line.

In the finite difference forms of equations (7), (8) and (10) that follow, it will be seen that special equations were required for points on the axis of the duct. For these equations, terms involving $(1/R)(\partial/\partial R)$, which in finite difference form cannot be directly evaluated at $R = 0$, were reduced to the form $\partial^2/\partial R^2$ by L'Hospital's rule.

Continuity equation:

When $0 < R < 1$:

$$\frac{2}{R_k + R_{k+1}}\left[\frac{V_{j,k+1}R_{k+1} - V_{j,k}R_k}{\Delta R}\right] + \frac{(U_{j,k+1} + U_{j,k}) - (U_{j-1,k+1} + U_{j-1,k})}{2\Delta X} = 0. \quad \text{(A1)}$$

When $R = 0$ and 1:

$$V_{j,k} = 0. \quad \text{(A2)}$$

Momentum equation:

When $0 < R < 1$:

$$U_{j-1,k}\left[\frac{U_{j,k} - U_{j-1,k}}{\Delta X}\right] + \left[V_{j-1,k} - \frac{1}{R_k}\right]\left[\frac{U_{j,k+1} - U_{j,k-1}}{2\Delta R}\right] = \left[\frac{U_{j,k+1} - 2U_{j,k} + U_{j,k-1}}{\Delta R^2}\right] - \left[\frac{P_{dj} - P_{dj-1}}{\Delta X}\right] + \theta_{j,k}. \quad \text{(A3)}$$

When $R = 0$:

$$U_{j-1,k}\left[\frac{U_{j,k} - U_{j-1,k}}{\Delta X}\right] + V_{j-1,k}\left[\frac{U_{j,k+1} - U_{j,k-1}}{2\Delta R}\right] = 2\left[\frac{U_{j,k} - 2U_{j,k} + U_{j,k-1}}{\Delta R^2}\right] - \left[\frac{P_{dj} - P_{dj-1}}{\Delta X}\right] + \theta_{j,k}. \quad \text{(A4)}$$

Energy equation:

When $0 < R < 1$:

$$U_{j-1,k}\left[\frac{\theta_{j,k} - \theta_{j-1,k}}{\Delta X}\right] + \left[V_{jk} - \frac{1}{Pr\,R_k}\right]\left[\frac{\theta_{j,k+1} - \theta_{j,k-1}}{2\Delta R}\right] = \frac{1}{Pr}\left[\frac{\theta_{j,k+1} - 2\theta_{j,k} + \theta_{j,k-1}}{\Delta R^2}\right]. \quad \text{(A5)}$$

When $R = 0$:

$$U_{j-1,k}\left[\frac{\theta_{j,k} - \theta_{j-1,k}}{\Delta X}\right] + V_{j,k}\left[\frac{\theta_{j,k+1} - \theta_{j,k-1}}{2\Delta R}\right] = \frac{2}{Pr}\left[\frac{\theta_{j,k+1} - 2\theta_{j,k} + \theta_{j,k-1}}{\Delta R^2}\right]. \quad \text{(A6)}$$

APPENDIX B

Solution by Relaxation

The finite difference equations, equations (A1)–(A6), were solved by a step-by-step relaxation procedure, which was initiated at the bottom of the duct for particular values of the dimensionless flow Q, and the Prandtl number, and for a specified inlet condition.

As the local wall temperature was unknown, it had to be determined together with the fluid temperature at the grid points on each relaxation row. An expression will now be derived that was used to obtain the surface temperature on a row. The heat transferred from inlet to elevation X is given by

$$H_x = 2\pi XF. \quad \text{(B1)}$$

Using equation (16) to replace F (dimensionless heat flux) in equation (B1) gives

$$H_x = \frac{2\pi X}{Pr} \quad \text{(B2)}$$

and combining equations (B2) and (12) yields

$$\frac{X}{Pr} = \int_0^1 U_x\theta_x R\,dR. \quad \text{(B3)}$$

Equation (B3) thus links the surface temperature with the fluid temperature. The relaxation procedure that was adopted is as follows:

1. Values were assigned to Q and Pr.
2. On the bottom row of the relaxation grid, Row 1, the pressure defect P_{d1}, and the velocities $U_{1,k}$, were set equal to the specified inlet conditions, the temperatures of the surface and the fluid were set equal to zero, and the radial velocities $V_{1,k}$, were set equal to zero.
3. On the second row:

   $U_{2,k}$ was initially set equal to $U_{1,k}$, and
   $\theta_{2,k}$ was initially set equal to $\theta_{1,k}$.
4. The momentum equation, equations (A2) and (A3), was relaxed for all fluid points on Row 2. Since $U_{2,k}$ and P_{d2} were both unknown at each point, the equation was relaxed for the variable

$$U_{2,k} + \left[\frac{P_{d2} - P_{d1}}{\Delta X}\right] \Big/ \left[\frac{U_{1,k}}{\Delta X} + \frac{C}{\Delta R^2}\right]$$

where $C = 2$ for $0 < R < 1$ and $C = 4$ for $R = 0$. As each point on Row 2 has the same value of P_{d2} (from equation (9)) the two variables were separated by using equation (11) in finite difference form.

5. The continuity equation, equations (A1) and (A2), was solved for grid points on Row 2 to give $V_{2,k}$. It is worth mentioning that although the continuity equation is of the first order no difficulties were encountered in obtaining sensible values of $V_{2,k}$ owing to the assumed axisymmetrical nature of the flow.
6. The energy equation, equations (A5) and (A6), were solved for all points in the fluid on Row 2 and then equation (B3) was solved to obtain a new estimate of the surface temperature. This procedure was repeated until all temperatures on Row 2 were satisfactorily relaxed.
7. Values of the variables on Row 3 and subsequent rows until P_d ceased to be negative were found in a similar way. Linear interpolation yielded the elevation at which P_d returned to zero; this elevation corresponded to the top of the duct.
8. The reciprocal of the dimensionless length of the duct yielded the Grashof number, and the Nusselt number was obtained from equation (19).

LE DEVELOPPEMENT DE LA CONVECTION NATURELLE LAMINAIRE DANS UNE CONDUITE VERTICALE AVEC FLUX DE CHALEUR CONSTANT

Résumé—On présente une étude théorique et expérimentale de l'écoulement laminaire en convection naturelle dans des conduites verticales chauffées. Les conduites ont une section droite circulaire; leurs extrémités sont ouvertes et leur surface interne dissipe uniformément la chaleur.

Les champs de vitesse et de température ainsi que la relation entre les nombres de Nusselt et de Rayleigh sont obtenus par la résolution des équations fondamentales à l'aide d'une technique numérique de pas à pas. Deux nombres de Rayleigh sont introduits, l'un est exprimé en fonction du flux thermique constant et l'autre en fonction de la température moyenne de paroi. L'influence du nombre de Prandtl sur la relation qui lie les nombres de Nusselt et de Rayleigh est discutée. Trois conditions à l'entrée sont examinées; elles ont toutes fourni la même expression du nombre de Nusselt pour les faibles nombres de Rayleigh, et les différences entre les expressions du nombre de Nusselt obtenues aux nombres de Rayleigh élevés ont été trouvées faibles.

Les nombres de Nusselt d'origine expérimentale, l'air étant utilisé comme fluide convectif, sont en accord satisfaisant avec les relations théoriques.

DIE AUSBILDUNG DER LAMINAREN, NATÜRLICHEN KONVEKTIONSSTRÖMUNG IN EINEM SENKRECHTEN ROHR MIT KONSTANTEM WÄRMESTROM

Zusammenfassung—Es wird über eine theoretische und experimentelle Studie der laminaren, freien Konvektionsströmung in senkrechten, beheizten Rohren berichtet. Die runden Rohre sind an beiden Enden offen und übertragen auf ihrer Innenseite einen konstanten Wärmestrom.

Die Temperatur- und Geschwindigkeitsfelder und die Beziehung zwischen den Nusselt- und Rayleigh-Zahlen wurden durch die Lösung der maßgebenden Gleichungen mit Hilfe eines numerischen Differenzenverfahrens ermittelt. Es werden zwei Rayleigh-Zahlen definiert: die eine auf der Basis des konstanten Wärmestroms und die andere mit der mittleren Wandtemperatur. Der Einfluß der Prandtl-Zahl auf die Nusselt- bzw. Rayleigh-Zahl wird erläutert. Drei verschiedene Einströmbedingungen wurden untersucht; Bei kleinen Rayleigh-Zahlen ergab sich dieselbe Nusselt-Beziehung, während bei großen Rayleigh-Zahlen nur kleine Differenzen in der Nusselt-Beziehung auftraten. Experimentell ermittelte Nusselt-Zahlen für Luft stimmen mit der theoretischen Beziehung zufriedenstellend überein.

РАЗВИТИЕ ЛАМИНАРНОГО СВОБОДНО-КОНВЕКТИВНОГО ТЕЧЕНИЯ В ВЕРТИКАЛЬНОМ КАНАЛЕ С ПОСТОЯННЫМ ПОТОКОМ ТЕПЛА

Аннотация — Представлены результаты теоретического и экспериментального исследования ламинарного свободно-конвективного течения в нагреваемых вертикальных каналах. Каналы круглого сечения, открытые с обоих концов и с постоянным потоком тепла на их внутренних поверхностях.

Из решения основных уравнений методом последовательных приближений численно получены поля температур и скорости и зависимости между числами Нуссельта и Релея. Вводятся два числа Релея: одно выражено через постоянный тепловой поток и другое — через среднюю температуру стенки. Обсуждается влияние числа Прандтля на отношение шежду числами Нуссельта и Релея. Исследовались три условия на входе; все они дали одну и ту же зависимость Нуссельта для малых чисел Релея и только малые разности между зависимостями Нуссельта для больших чисел Релея.

Экспериментально найденные значения чисел Нуссельта для воздуха в качестве конвектирующей среды хорошо согласуются с теоретическими результатами.